

Nanotubular J-Aggregates Coated by Transparent Silica Nanoshells

Yan Qiao,^{a,b†1} Frank Polzer,^{a,‡2} Holm Kirmse,^a Stefan Kirstein,^{a*} Jürgen P. Rabe^{a,b}*

^a Department of Physics, Humboldt-Universität zu Berlin, Newtonstr 15, 12489 Berlin, Germany. ^b IRIS Adlershof, Humboldt-Universität zu Berlin, Zum Großen Windkanal 6, 12489 Berlin, Germany.

KEYWORDS: Organic-inorganic hybrid · sol-gel · photostability · fluorescence spectroscopy · Cryo-TEM · light harvesting complexes

NOTES: The authors declare no competing financial interest.

TITLE RUNNING HEAD: Silica shell of tubular J-aggregates

¹ present address: Centre for Protolife Research and Centre for Organized Matter Chemistry, School of Chemistry, University of Bristol, Bristol BS8 1TS, United Kingdom

² present address: Materials Science & Engineering, University of Delaware, Newark, DE 19716, USA.

ABSTRACT

Nanotubular J-aggregates of amphiphilic cyanine dyes exhibit highly attractive opto-electronic properties, reminiscent to natural light harvesting complexes. However, their photo-chemical and mechanical stabilities are limited. A robust transparent shell covering the J-aggregates may alleviate these issues. Here, organic-inorganic hybrid nanotubes have been synthesized based on *in-situ* coating the nanotubular J-aggregates with silica through the sol-gel method. The growth of the shell is controlled by electrostatic adsorption of the silica precursors. The resulting silica nanoshells exhibit a regular superstructure that consists of ribbons that helically wind around the tubular aggregates. The molecular structure of the aggregates and hence their spectral properties remain unaffected by the silication process. The overall shell thickness can be controlled by the ratio and the absolute concentration of the precursors. The usage of a precursor containing diamine groups leads to the formation of bundles of the tubular aggregates that are covered by silica. The nanometer sized silica shell offers advantages with regard to photostability, higher mechanical stiffness, and increased chemical inertness which facilitates optical investigations and further applications.

FULL TEXT

Ordered clusters of molecular dyes, such as J-aggregates, have long sparked much interest^{1, 2} due to their peculiar optical properties, such as intensive, narrow, and, with respect to their monomers, red shifted absorption bands, a nearly resonant narrowband fluorescence emission, and strong exciton delocalization and migration. Owing to these characteristics, J-aggregates have been used as light sensitizers in film photography³ and

nanoscale materials for electronic excitation energy collection and transport.^{4, 5} Recently, tubular J-aggregates formed by amphiphilic cyanine dyes have attracted significant attention^{6, 7} since they can serve as model systems for artificial nanostructures to mimic chlorosomal light-harvesting (LH) complexes of green sulfur and non-sulfur bacteria, which are known to exhibit the highest LH efficiency.⁸ Similar to the natural LH centers, the tubular J-aggregates are comprised of dyes and display double-walled tubular structures with well-defined molecular orientations.⁹ Owing to the highly ordered molecular stacking and coherent coupling, the tubular J-aggregates are anticipated to pave the way towards fast excitation energy transfer, enabling the investigation of energy migration and charge transfer processes observed in nature.⁷ However, the investigation and application of these J-aggregates has posed a long-standing challenge due to their poor stability at elevated temperatures or extreme pH values, low photostability, and weak mechanical strength. Therefore, a method that leads to increase the mechanical and photochemical stability of the J-aggregates in solution is desirable.

Hybrid materials of silica and functional organic building blocks have intrigued intensive investigation, because of the optical transparency of silica in combination with biocompatibility, structural robustness, improved environmental stability, and feasibility of chemical modification.^{10, 11} The combination of inorganic silica and organic J-aggregates is therefore particularly promising. Typical examples studied so far include silica sphere encapsulated J-aggregates or silica/J-aggregate films¹². An interesting work by S. Mann *et al.* has reported template-directed synthesis of silica-coated porphyrin J-aggregate nanotapes exhibiting retention of the optical properties.¹³ Within the silica host matrix, the optical properties of the J-aggregate could be modulated by tuning the

coupling to localized plasmons.¹⁴ Inspired by these previous results, we present a route to synthesize silica nanoshells onto nanotubular J-aggregates in the hope of enhancing their photostability while preserving the optical properties of the J-aggregates. Moreover, the formation of a silica shell *via* the sol-gel method seems to transcript the morphology of the J-aggregate nanotubes into inorganic silica, which is expected to provide additional structural information about the J-aggregates. Previous work from our group has proposed that amphiphilic cyanine dyes adopt a helical arrangement inside the J-aggregate bilayers¹⁵; however, this hypothesis was so far only supported by direct imaging technique (e.g., electron microscopy) with quite low contrast of the organic molecules. In this work, structural replicas of tubular J-aggregates into silica materials *via* sol-gel process are obtained that provide strong indication for a helical arrangement of the cyanine dyes within the tubular wall.

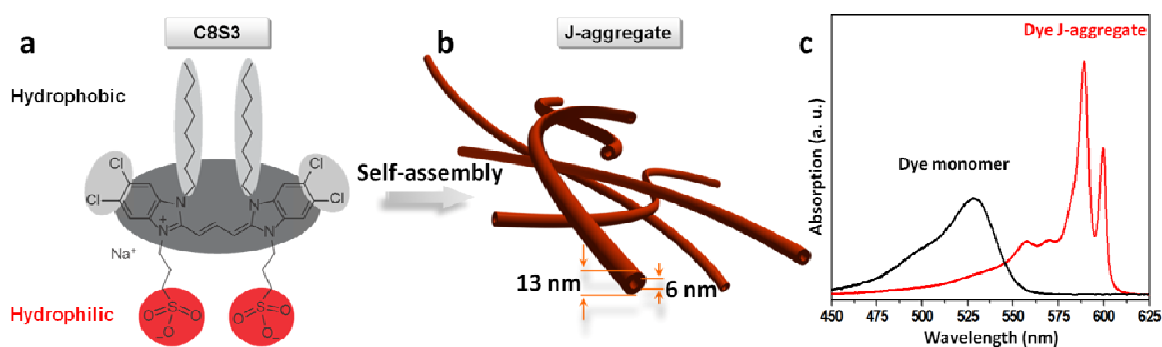


Figure 1. Sketch of molecular self-assembly into J-aggregates. (a) Molecular structure of amphiphilic cyanine dye C8S3; (b) sketch of nanotubular J-aggregates; (c) absorption spectra of C8S3 monomer (black) and J-aggregate (red) solution, in which J-aggregates exhibit narrow and red-shifted absorption peaks relative to monomers.

Cyanine dye 3,3'-bis(2-sulfopropyl)-5,5',6,6'-tetrachloro-1,1'-dioctylbenzimidacarbocyanine (C8S3, Fig. 1a) is known to self-assemble into nanotubular J-aggregates in a water/methanol solution (100/13, v/v).¹⁶ The resulting J-aggregates are double-walled nanotubes with an outer diameter of 13 ± 1 nm, an inner diameter of 6.5 ± 1 nm, and lengths up to tens of micrometers (Fig. 1b). These structural features make the J-aggregate nanotube an excellent model system for the LH complex in nature. The UV-vis spectra show a large red-shift upon the formation of the J-aggregate (Fig. 1c). Using these supramolecular nanotubes as supporting scaffolds, optical transparent helical silica nanoshells are prepared through the sol-gel process with aminopropyltriethoxysilane (APTES), trimethoxysilylpropylethylenediamine (TMSPEA), and tetraethoxysilane (TEOS) as silica precursors. In a typical process, 2 μ L of APTES methanol (v/v = 1:49) solution and 15 μ L TEOS methanol (v/v = 1:49) solution was added to a 250 μ L C8S3 J-aggregate solution. The final concentration of APTES and TEOS are 0.684 mM and 5.37 mM, respectively. The solution was vortexed to ensure complete mixing and stored for 24 hours before measurement.

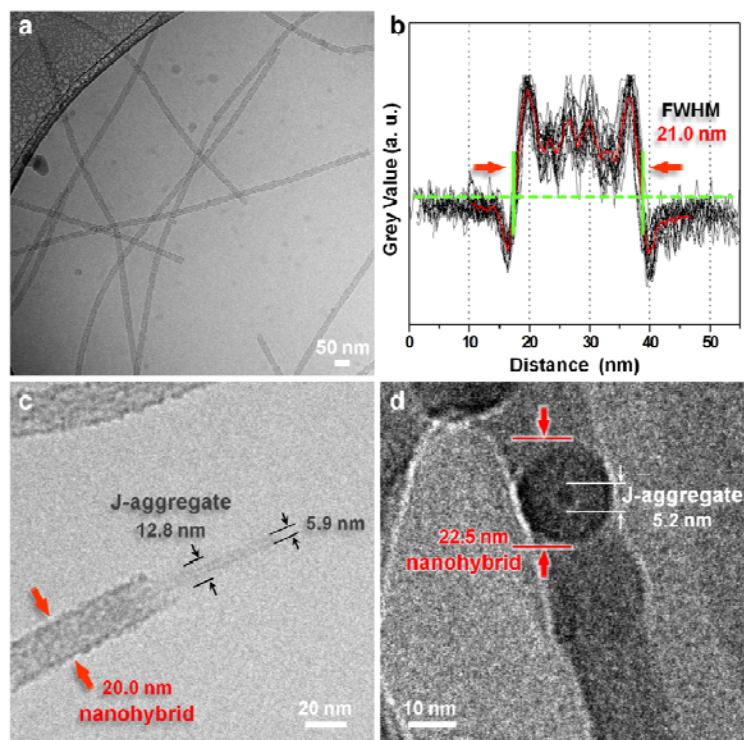


Figure 2. Cryo-TEM images and analysis of silica helical nanoshell coated J-aggregates. (a) An overview of nanohybrids. (b) Overlaid line scans across different individual nanohybrids reflecting the highly structural homogeneity. The red curve is the average curve which displayed the average diameter was 21 ± 1.5 nm. The four peaks in the red curve proved the repeated periods of the helical silica nanoshells. (c) An end section of the nanohybrid denoting the remaining of the original tubular J-aggregate. (d) An upstanding nanohybrid indicating the inner tube was filled by silica.

Cryogenic transmission electron microscopy (cryo-TEM) was employed to visualize the silica-coated J-aggregates in an *in-situ* state.¹⁵ As shown in Fig. 2a, thread-like structures which are deemed as silica nanoshell coated J-aggregate hybrids were obtained. Cross-sectional line profiles were taken across the nanohybrids as presented in Fig. 2b. An overlay of line scans taken from different hybrid tubes resolved the average diameter

of the nanohybrids to be 21 ± 1.5 nm, as measured by the full width at half maximum (FWHM). The line scans show similar diameters manifesting the homogeneity of the hybrid nanotubes. Compared to the diameter of the J-aggregate template of 13 ± 1 nm the mean diameter of silica coated J-aggregates has increased by 7 to 8 nm. If this increase is assigned to a silica shell solely, the shell has a mean thickness of 3.5 to 4 nm. The growth of the silica shell on the outer surface of tubular J-aggregates is further clarified by Fig. 2c. An end section of the nanohybrid is shown in a magnified view. One can see the remaining of the original tubular J-aggregate as it protrudes from the silica shell. The diameter of the J-aggregate tube is of the same dimensions as observed for aggregates of pure dye solutions (13 nm of outer diameter and 6.5 nm for inner diameter).⁷ Obviously, the sol-gel process does not cause significant changes in morphology or size of the J-aggregate nanotubes. This is further supported by optical spectroscopy, as shown below. In Fig. 2d, a top view of the open end of an upstanding nanohybrid is displayed, which was found accidentally. The center of the tube is filled with a dark spot that may be identified as filling of the tube with silica. The diameter is close to what was previously measured for the pure aggregates filled with silver.¹⁷ It is interesting to note here, that no contrast is seen between the organic wall of the J-aggregate and the silica shell.

As verified in Fig. S1 (Supporting Information), the nanohybrids with a high product yield can extend in length up to tens of micrometers. Negligible amounts of non-templated silica were retained. It is important to note that no obvious bundling effect of the J-aggregate is observed after the silication with APTES/TEOS and most of the nanohybrids are isolated. Additionally, although the resulting silica coated nanohybrids are flexible, the deposition of the silica nanoshells increased the stiffness of the nanotubes,

as can be seen from the typical increase of bending radius. Energy dispersive X-ray spectroscopy (EDXS, Fig. S2) strongly supports that the nanostructures are comprised of J-aggregate (origin of S-signal) and silica (origin of Si-signal).

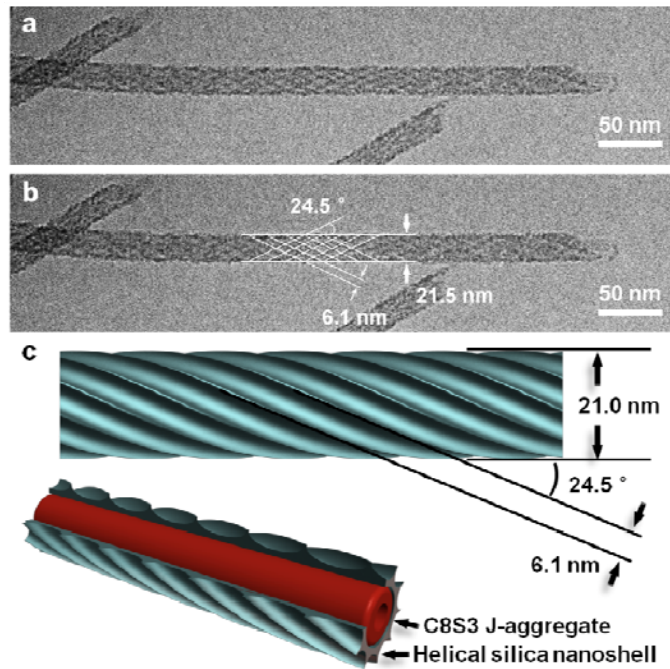


Figure 3. (a) Cryo-TEM image of silica nanoshell coated J-aggregates. (b) A detailed analysis of the superstructure. (c) 3D model of the surface and cross-section of silica coated J-aggregates exhibiting the parameters of helical structures.

In a magnified cryo-TEM image (Fig. 3a), a typical silica/J-aggregate nanohybrid revealed a well-ordered net-like pattern which is indicative for a repetitive pattern expected from the projection image of a helical structure. A close inspection reveals the width of the ribbons that constitute the helix is 6.1 nm with a tilt angle of 24 degree (Fig. 3b). The helical handedness, however, cannot be identified from the projection images obtained by cryo-TEM. A sketch of a 3D model of the nanohybrids using the helical

parameters extracted from Fig. 3b is shown in Fig. 3c. It is important to note that the width of these ribbons as well as the tilt angle differ from the values proposed for the pure J-aggregates¹⁵, which means, the silica super structure is not a direct one-to-one transcript of the aggregate structure.

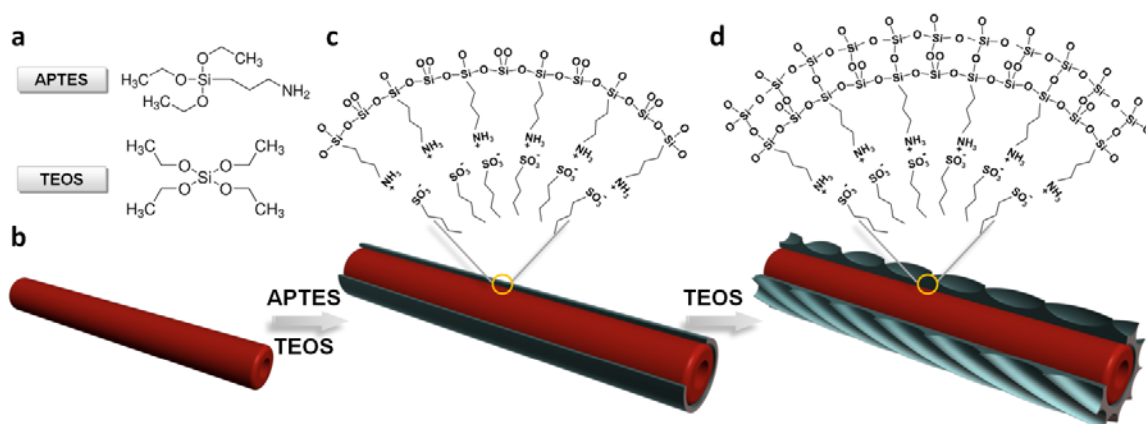


Figure 4. Sketch of electrostatically driven silylation of tubular J-aggregate. (a) Molecular structures of the constituents: APTES, and TEOS; (b) sketch of J-aggregate nanotube, (c) electrostatic adsorption of APTES on J-aggregates; (d) condensation of TEOS on J-aggregate nanotubes.

The formation of the silica nanoshell is initiated and driven by electrostatic forces and requires charge matching between silica precursor and template (Fig. 4).^{18, 19} The surface of the tubular J-aggregates is assumed to be negatively charged due to the sulfonate groups of the C8S3 anions. The cationic species, such as $[\text{Si}(\text{OH})_3(\text{NH}_3)]^+$ hydrolyzed from APTES, are attracted by the negative surface potential and form an ultrathin silica layer. Further condensation of hydrolysis products of TEOS, e. g. $[\text{Si}(\text{OH})_4]$, leads then to the formation of silica nanoshell specifically on those parts of the

J-aggregate surface that were previously covered by APTES. It is supposed that the silica nanoshell can inherit and amplify small corrugations of the aggregate surface. Therefore, the proposed helical superstructure of the tubular aggregates seems to induce helicity to the silica layer.

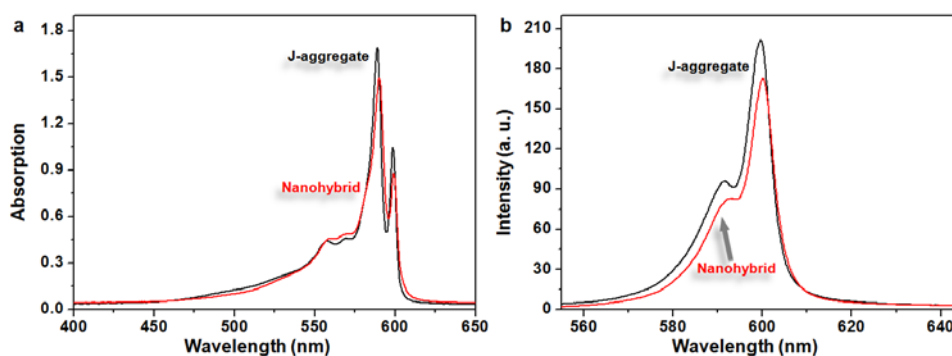


Figure 5. Optical characterizations of nano hybrid and J-aggregates. (a) Absorption spectra; (b) PL spectra of as-prepared nano hybrid and J-aggregate before photo bleaching ($\lambda_{ex}=500$ nm).

The optical properties of the silica coated J-aggregates were investigated by UV-vis and fluorescence measurements. Comparison of UV-vis spectra of nano hybrid (red line) with the pure J-aggregates solution (black line) (Fig. 5a), shows no significant change. Obviously, the encapsulation of the J-aggregates by silica does not lead to heavy reorganization of the J-aggregate structure. Only a slight broadening of the main peaks at 599 and 589 nm is observed in combination with a slight relative increase of the absorbance at the transition bands at around 550 - 570 nm. These slight changes may be either due to very slight structural changes or different polarity of the close environment of the dyes due to presence of silica. It is important to note here, that from our TEM data

we are convinced that all aggregates are covered by silica. Therefore, the slight changes cannot be explained by changes of only a small fraction of J-aggregates. Fig. 5b illustrates uncorrected fluorescence spectra showing that the intensity of silica nanoshell-coated J-aggregates has slightly decreased compared to the bare ones. However, the fluorescence quantum yield (Φ_f) is approximately 13% higher for silica nanoshell-coated J-aggregate, i.e. $\Phi_f = 8\%$ for silica nanoshell-coated J-aggregates versus 6% for bare J-aggregates (Fig. S3).

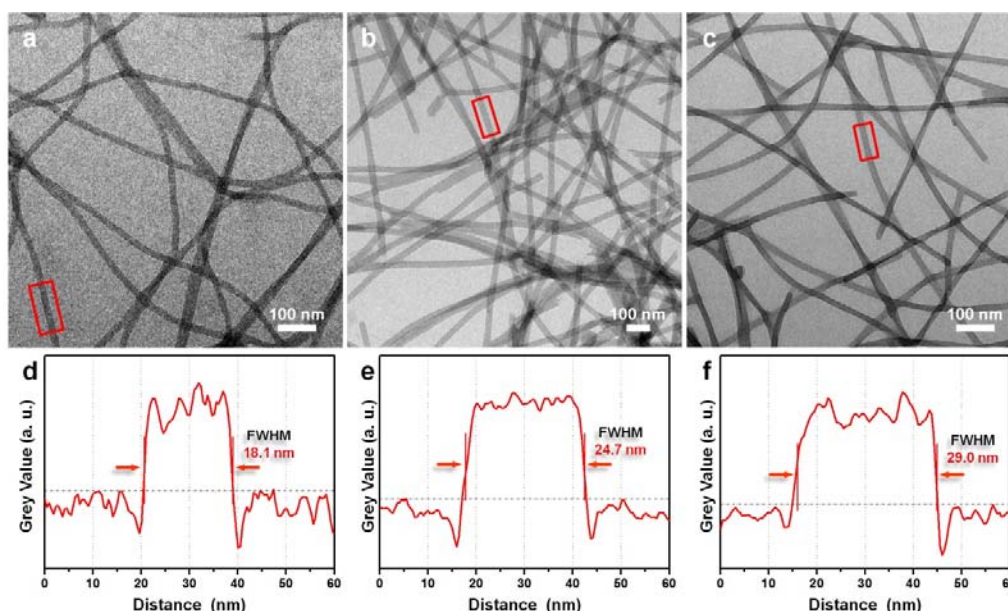


Figure 6. TEM images (a-c) and line scans (d-f) of silica coated nanohybrids prepared with different ATPES/TEOS concentration. (a, d) 0.684 mM / 3.58 mM; (b, e) 0.684 mM / 10.7 mM and (c, f) 0.684 mM / 14.3 mM.

The thickness of the silica nanoshell can be facily adjusted by varying the concentration of the silica precursor. For instance, the thickness of the silica nanoshell on the J-aggregate increases as the TEOS concentration is raised. As Fig. 6 shows, the total

diameter of the nanohybrid is 18.1 nm giving a thickness of the silica shell of around 2.5 nm when the concentration of TEOS is decreased to 3.58 mM. Further doubling of the TEOS concentration to 10.7 mM increases the nanohybrid diameter to 24.7 nm and the thickness of inorganic layer to 5.9 nm. When the TEOS concentration reaches to 14.3 mM, the nanotube diameter increases to 29.0 nm and the silica layer thickness is 8.0 nm. It is therefore believed that this method is a straightforward, effective, and adaptive way to synthesize silica nanoshell coated nanohybrids of defined thickness.

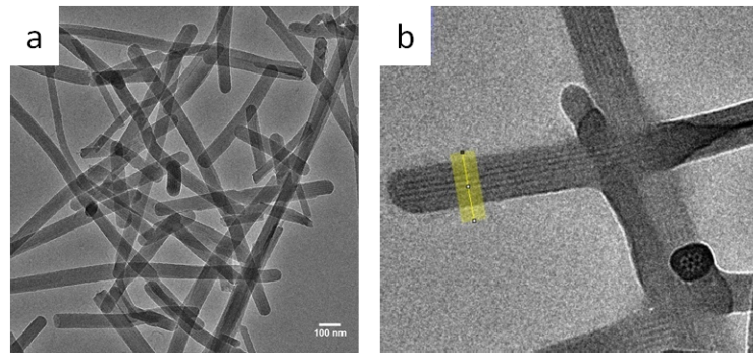


Figure 7. TEM images (a) and cryo-TEM image (b) of TMSPEA/TEOS covered bundles of tubular aggregates. In (b) a view on the face side of a bundle is seen. The periodicity of the stripes in (a) is 8.7 ± 0.5 nm, the mean distance between the dark centers of the tubes in (b) 10.5 ± 0.3 nm.

A different behavior was found when N-[3-(trimethoxysilyl)propyl]ethylenediamine (TMSPEA) was used as precursor instead of APTES. TEM images (Fig. 7a) reveal bulkier rod-like objects that are identified by cryo-TEM (Fig. 7b) as bundles of tubular aggregates. Those bundles have been described earlier¹⁵ and they emerged by random agglomeration or were induced by addition of cations.⁶ In contrast to prior experimental

reports⁶, the overall diameter of the bundles, and hence the number of tubes involved to form a bundle, is rather homogeneous. Additionally, the bundles are almost straight which indicates high stiffness, and no twisting of the single tubes within one bundle is observed. An important observation is the decrease of the diameter of a single tube within the bundle. In a serendipitously found image (Fig. 7b) a top view of the face of a bundle is found. Clearly the hexagonal arrangement of dark black spots is seen surrounded by a dark boundary. The bright white line is due to the defocus of the TEM. The dark spots are interpreted as silica filling the inner part of the tubes. The mean distance between the centers of these spots is $d = 10.5 \pm 0.3$ nm. The periodicity of the stripes of bundles observed from the side view is 8.7 ± 0.5 nm, which fits well to $\sqrt{3}/2 \cdot d$, the distance between lines of dots in the top-view of Fig. 7b. The reduction of diameter from 13 ± 0.5 nm to 10.5 ± 0.3 nm was also reported earlier⁶ and explained by a rearrangement of the tubular aggregate structure where the bilayer structure of the original tube is converted into a single layer structure. This model is fully confirmed by our findings: first, because of the dimensions of the bundled aggregate, second, because of the fact the inner space of the tube is filled by silica which is due to the electrostatic attraction of the cationic precursors by the anionic dyes.

In preliminary experiments, it was found that the silica nanoshell stabilizes the J-aggregate against photobleaching. Since photobleaching of cyanine dyes is known to be caused by the reaction with singlet oxygen or by reaction with hydroxyl radicals, we conclude that the silica nanoshell is dense enough to significantly reduce the penetration of such radicals. However, the temporal behavior of photobleaching varied between

individual samples, probably due to residual porosity or structural variations not seen directly by the cryo-TEM images.

In conclusion, *in-situ* synthesis of silica nanoshells on tubular J-aggregates was realized based on the electrostatic attraction between silica precursors and the J-aggregates. The resulting nanohybrids exhibit a regular superstructure that may be induced by the supramolecular helical structure of the J-aggregates. The nanometer sized silica shell offers the advantages of improved photostability and higher mechanical stiffness, which should facilitate applications, such as artificial photosynthetic reactions up to water splitting and carbon dioxide fixation. This hybrid nanomaterial also offers improved stability against temperature and various chemical environments, and facilitates processability. Moreover, the interaction between the J-aggregate and the silica nanoshell should be an interesting subject to better understand the amazing properties of natural chlorophylls or enzymes.²⁰

Supporting Information.

In the supporting information, materials and methods, TEM, HRTEM images of nanohybrids, EDXS analysis of nanohybrids, measurement of fluorescence quantum yields of J-aggregate with and without silica shell, preliminary photo bleaching experiments are presented.

Acknowledgements

We thank Dr. Omar Al-Khatib and Evi Poblenz for fruitful discussions and assistance, respectively, and we acknowledge funding of the DFG through CRC 951. Dr. F. Polzer acknowledges funding also through the Joint Lab for Structural Research Berlin within IRIS Adlershof.

References

- 1 T. Kobayashi, *J-Aggregates*, World Scientific, Singapore, 1996.
- 2 F. Wuerthner, T. E. Kaiser and C. R. Saha-Moeller, *Angew. Chem.Int. Ed.*, 2011, **50**, 3376-3410.
- 3 T. Tani, *Photographic Sensitivity*, Oxford University Press, Oxford, UK, 1995.
- 4 G. D. Scholes, G. R. Fleming, A. Olaya-Castro and R. van Grondelle, *Nat. Chem.*, 2011, **3**, 763-774.
- 5 G. D. Scholes and G. Rumbles, *Nat. Mater.*, 2006, **5**, 683-696.
- 6 D. M. Eisele, J. Knoester, S. Kirstein, J. P. Rabe and D. A. Vanden Bout, *Nat. Nanotechnol.*, 2009, **4**, 658-663.
- 7 D. M. Eisele, D. H. Arias, X. Fu, E. A. Bloemsma, C. P. Steiner, R. A. Jensen, P. Rebentrost, H. Eisele, A. Tokmakoff, S. Lloyd, K. A. Nelson, D. Nicastro, J. Knoester and M. G. Bawendi, *Proc. Natl. Acad. Sci. U. S. A.*, 2014, **111**, E3367-E3375.
- 8 T. S. Balaban, H. Tamiaki and A. R. Holzwarth, in *Supramolecular Dye Chemistry*, ed. F. Wurthner, 2005, pp. 1-38.
- 9 C. Didraga, A. Pugzlys, P. R. Hania, H. von Berlepsch, K. Duppen and J. Knoester, *J. Phys. Chem. B*, 2004, **108**, 14976-14985.
- 10 S. Che, A. E. Garcia-Bennett, T. Yokoi, K. Sakamoto, H. Kunieda, O. Terasaki and T. Tatsumi, *Nat. Mater.*, 2003, **2**, 801-805.
- 11 Y. Qiao, H. Chen, Y. Lin, Z. Yang, X. Cheng and J. Huang, *J. Phys. Chem. C*, 2011, **115**, 7323-7330.
- 12 H. S. Zhou, T. Watanabe, A. Mito, I. Honma, K. Asai, K. Ishigure and M. Furuki, *Mater. Sci. Eng., B*, 2002, **95**, 180-186.
- 13 P. J. Meadows, E. Dujardin, S. R. Hall and S. Mann, *Chem. Commun.*, 2005, 3688-3690.
- 14 K. L. Gurunatha and E. Dujardin, *J. Phys. Chem. C*, 2013, **117**, 3489-3496.
- 15 H. v. Berlepsch, K. Ludwig, S. Kirstein and C. Boettcher, *Chem. Phys.*, 2011, **385**, 27-34.
- 16 H. von Berlepsch, S. Kirstein, R. Hania, A. Pugzlys and C. Boettcher, *J. Phys. Chem. B*, 2007, **111**, 1701-1711.
- 17 D. M. Eisele, H. V. Berlepsch, C. Bottcher, K. J. Stevenson, D. A. V. Bout, S. Kirstein and J. P. Rabe, *J. Am. Chem. Soc.*, 2010, **132**, 2104-2105.

- 18 A. Monnier, F. Schuth, Q. Huo, D. Kumar, D. Margolese, R. S. Maxwell, G. D. Stucky, M. Krishnamurty, P. Petroff, A. Firouzi, M. Janicke and B. F. Chmelka, *Science*, 1993, **261**, 1299-1303.
- 19 Y. Wan and D. Zhao, *Chem. Rev.*, 2007, **107**, 2821-2860.
- 20 T. Itoh, K. Yano, Y. Inada and Y. Fukushima, *J. Am. Chem. Soc.*, 2002, **124**, 13437-13441.

Nanotubular J-aggregates coated by transparent silica nanoshells

Yan Qiao,^{a,b†3} Frank Polzer,^{a,‡4} Holm Kirmse,^a Stefan Kirstein,^{a*} Jürgen P. Rabe^{a,b}*

^a Department of Physics, Humboldt-Universität zu Berlin, Newtonstr 15, 12489 Berlin, Germany. ^b IRIS Adlershof, Humboldt-Universität zu Berlin, Zum Großen Windkanal 6, 12489 Berlin, Germany.

KEYWORDS: Organic-inorganic hybrid · sol-gel · photostability · fluorescence spectroscopy · Cryo-TEM · light harvesting complexes

NOTES: The authors declare no competing financial interest.

TITLE RUNNING HEAD: Silica shell of tubular J-aggregates

³ present address: Centre for Protolife Research and Centre for Organized Matter Chemistry, School of Chemistry, University of Bristol, Bristol BS8 1TS, United Kingdom

⁴ present address: Materials Science & Engineering, University of Delaware, Newark, DE 19716, USA.

Supporting Information

1. Materials and Methods

Preparation of tubular J-aggregates. Double-walled J-aggregate nanotubes were prepared in water/methanol (9:1, v/v). Stock solution of C8S3 (2.92 mM) was prepared by directly dissolving C8S3 powder (FEW Chemicals, Germany) in methanol ($\geq 99.9\%$ GC, Sigma-Aldrich). Then 130 μL of the C8S3 stock solution was added to 500 μL of ultrapure H_2O followed by thorough vortex to ensure complete mixing. An immediate color change of the solution (from orange to deep pink) was observed, indicating the formation of tubular J-aggregates. The solution was stored in the dark for 24 h before adding an additional 500 μL of ultrapure H_2O , which gave a final concentration of 0.336 mM. Fresh J-aggregate solutions were stored in the dark and used within three days after preparation.

Preparation of silica nanoshell on the C8S3 J-aggregate. In a typical process, 2 μL of APTES methanol (v/v = 1:49) solution and 15 μL TEOS methanol (v/v = 1:49) solution was added to a 250 μL C8S3 J-aggregate solution. The solution was vortexed to ensure complete mixing and stored for 24 hours before measurement. All the experiments were finished under red light and the samples were stored in dark to protect from photobleaching.

Absorption spectroscopy. Absorption spectra of the solution were taken with a double-beam UV-vis spectrometer (Shimadzu UV-2101PC, Duisberg, Germany) in a 0.2 mm, 1.0 mm, or 10.0 mm demountable quartz cell (Hellma GmbH, Germany).

Fluorescence spectroscopy. Fluorescence spectra were taken on a fluorescence spectrometer (JASCO FP 6500) in quartz cells (Hellma GmbH, Germany) with the path length of 0.2 mm, 1.0 mm, or 10.0 mm. The fluorometer came with built-in light-source (Xe-lamp UXL-159, 150W), two grating-monochromators with variable slit-width and detector.

Cryo-genic transmission electron microscopy (Cryo-TEM). Droplets of the solution (5 μ L) were applied to carbon film (1 μ m hole diameter) covered 200 mesh grids (R1/4 batch of Quantifoil Micro Tools GmbH, Jena, Germany), which had been hydrophilized before use by plasma process. Supernatant fluid was removed by Vitrobot Mark II (FEI company, Eindhoven, Netherlands) until an ultrathin layer of the sample solution was obtained spanning the holes of the carbon film. The samples were immediately vitrified by propelling the grids into liquid ethane at its freezing point (90 K). Frozen samples were transferred into a JEOL JEM2100 (JEOL, Eching, Germany) using a Gatan 914 high-tilt cryo-transfer holder and Gatan work station (Gatan, Munich, Germany). Microscopy was carried out at a 94 K sample temperature using the microscope's low-dose protocol at an accelerating voltage of 200 kV (LaB6-illumination). The defocus was chosen to be approx 2 μ m to create sufficient phase contrast for imaging. Image analysis was performed with Image J software¹.

High Resolution Transmission Electron Microscopy (HR-TEM). High resolution transmission electron microscopy (TEM) was performed with a JEOL 2010F operating at 200 kV. Droplets of the sample (5 μ L) were applied to carbon film coated 200 mesh grids (Quantifoil Micro Tools GmbH, Jena, Germany), which had been hydrophilized before use by simply storing the grids over a water bath for a day. The excess fluid was removed

with a filter paper to form an ultra-thin layer on the carbon film. Image analysis was performed with Image J software¹.

2. TEM image of silica nanoshell coated J-aggregate hybrids.

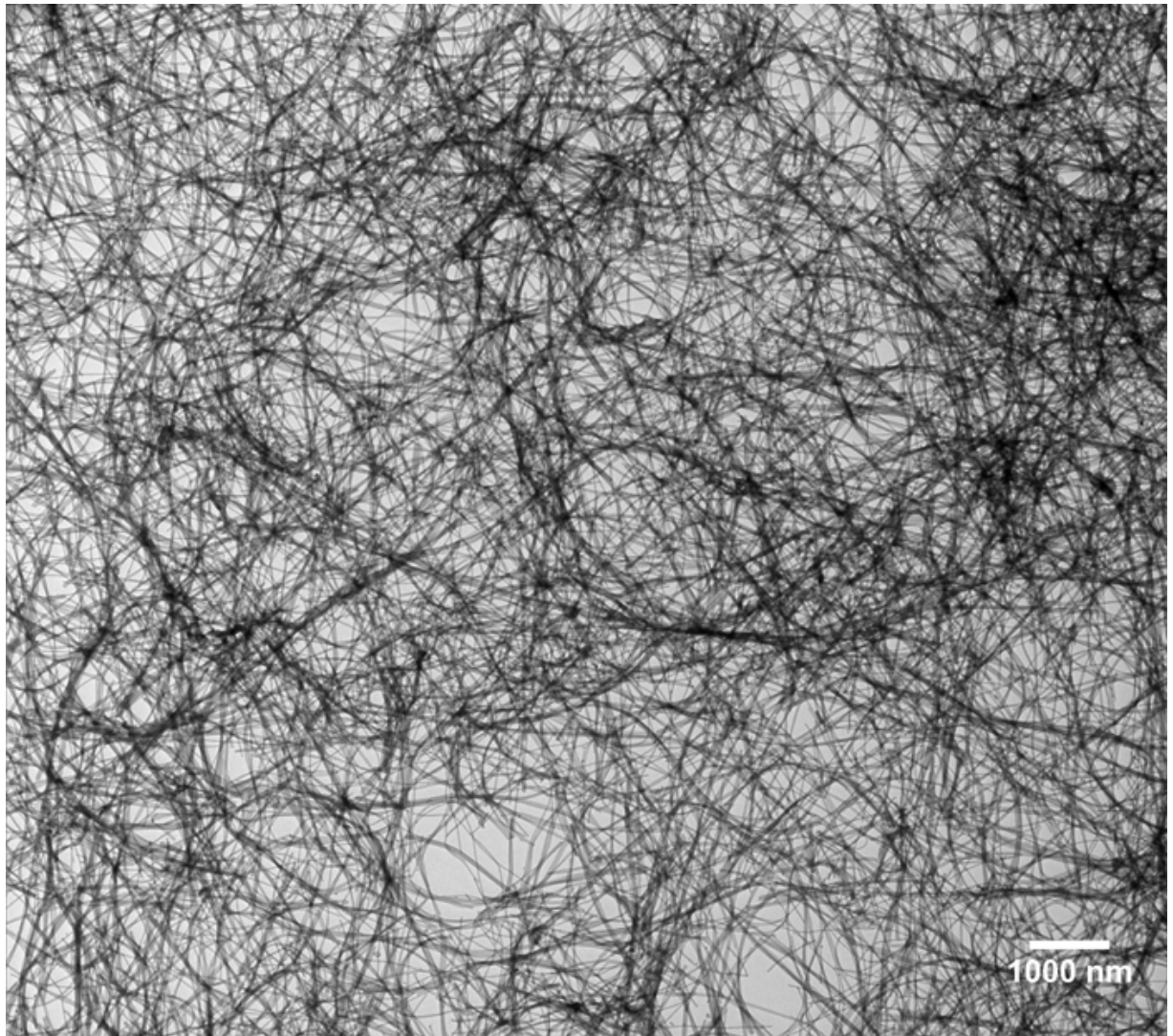


Figure S1. TEM image of silica nanoshell coated J-aggregate nano hybrids. The image shows tubular nano hybrids are several micrometers long.

3. HRTEM image of silica nanoshell coated J-aggregate hybrids.

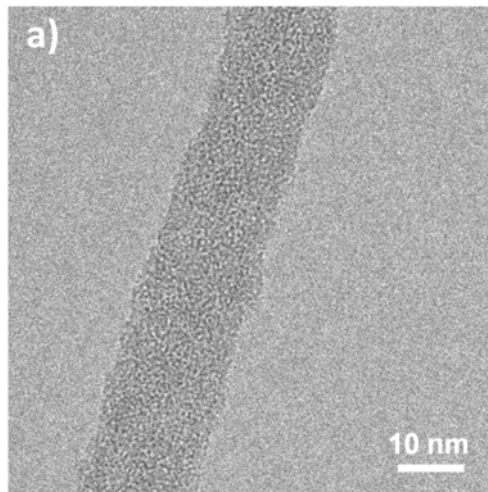


Figure S2. HR-TEM image of the as-prepared silica nanoshell-coated J-aggregate showing porous amorphous structure.

4. EDXS analysis of silica nanoshell coated J-aggregate hybrids.

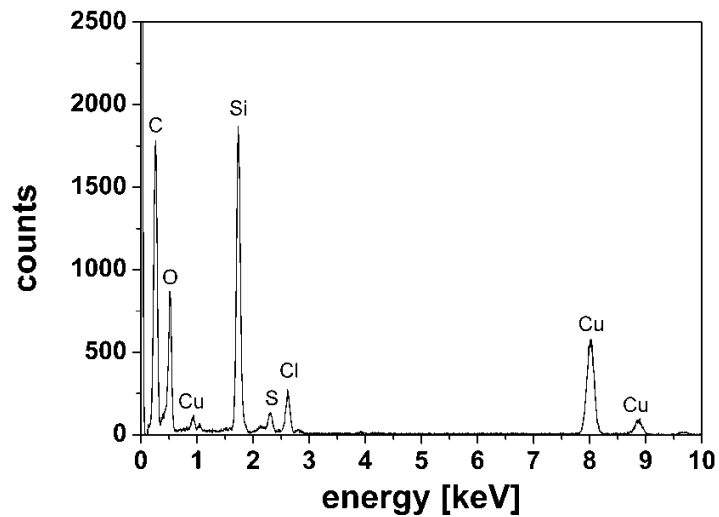


Figure S3. EDXS analysis of the as-prepared silica nanoshell-coated J-aggregate nanohybrids confirms the presence of Si and S elements.

5. Measurement of fluorescence quantum yields of J-aggregate with and without silica shell.

The fluorescence quantum yield (Q) is obtained using the comparative method of Williams *et al.*, which involves the use of well characterized standard fluorophore with known Q values. The quantum yield of the test sample is calculated using:

$$Q_X = Q_{ST} \left(\frac{I_X}{I_{ST}} \right) \left(\frac{OD_{ST}}{OD_X} \right) \left(\frac{\eta_X^2}{\eta_{ST}^2} \right)$$

Where the subscripts ST and X denote standard and test respectively, Q is the fluorescence quantum yield, I is the integrated fluorescence intensity, η is the refractive index, and OD is the optical density. In this work, a series of solutions were prepared with optical densities between 0.1 and 0.01, and a more accurate method was used to determine Q by the following formula:

$$Q_X = Q_{ST} \left(\frac{Grad_X}{Grad_{ST}} \right) \left(\frac{\eta_X^2}{\eta_{ST}^2} \right)$$

where $Grad$ is the gradient obtained from the plot of integrated fluorescence intensity I versus the absorbance. Fluorescein in 0.1 M NaOH solution ($Q = 95\%$)² Rhodamine B ($Q = 31\%$)³ was used as a standard sample for J-aggregate. All the fluorescence spectra were recorded with constant slit widths. The obtained quantum yields of J-aggregate with and without silica shell were 8%, and 6%, respectively.

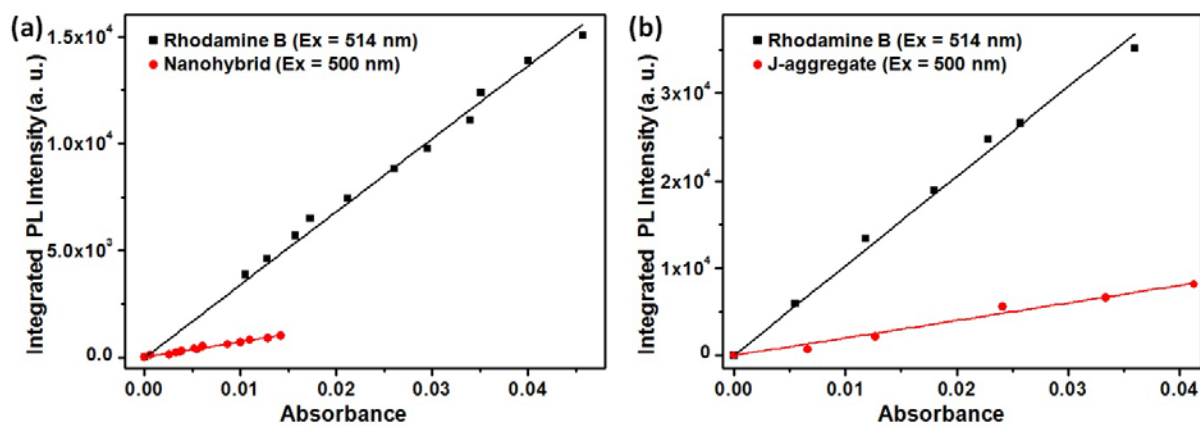


Figure S4. Linear plots of the measured absorption and integrated fluorescence intensity of: (a) rhodamine B and C8S3 J-aggregate; (b) rhodamine B and silica nanoshell-coated C8S3 J-aggregate.

6. Preliminary Photo bleaching experiments.

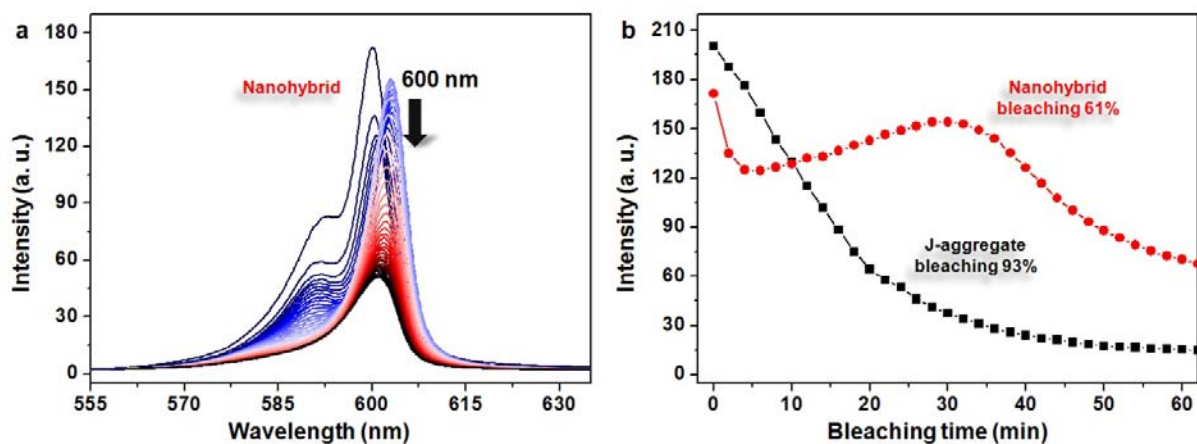


Figure S5. PL spectra of nanohybrids recorded under radiation with Xe lamp (from fluorescence spectrometer), spectra taken at time intervals of 2 min ($\lambda_{\text{ex}} = 500$ nm). (d) PL intensity at 600 nm versus photo bleaching time.

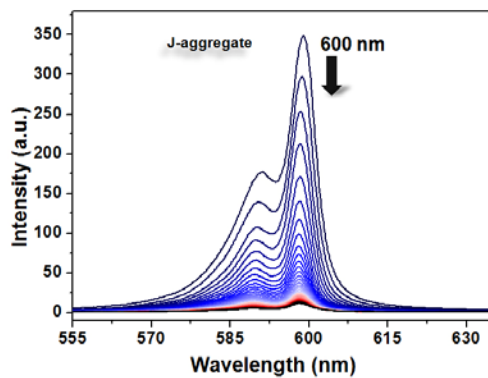


Figure S6. Photo bleaching of pure J-aggregate solution, recorded under same conditions as in Figure 5.

Spread sheet for preparation of samples:

	A	B	C	D	E
1					
2	250 μ L C8S3 J-aggregate solution				
3	J-agg concentration	0.000336 M			
4	J-agg volume	0.00025 L			
5	Mol of J-agg	0.000000084 mol			
6					
7	2 μ L of APTES methanol (v/v = 1:49) solution				
8	APTES volume	0.002 mL			
9	ratio	0.02			
10	density	0.946 g/mL at 25 °C(lit.)			
11	Molecular Weight	221.37 g/mol			
12	Mol of APTES	1.70936E-07 mol			
13	Concentration of APTES	0.000683742 M		6.84E-01 mM	
14	compare to J-agg	2.034946878		2	
15					
16	15 μ L TEOS methanol (v/v = 1:49) solution				
17	TEOS volume	0.015 mL			
18	ratio	0.02			
19	density	0.933 g/mL at 20°C			
20	Molecular Weight	208.33 g/mol			
21	Mol of TEOS	1.34354E-06 mol			
22	Concentration of TEOS	0.005374166 M		5.37E+00 mM	
23	compare to J-agg	15.99454163		16	

References

- 1 W. S. Rasband, ImageJ, <http://imagej.nih.gov/ij/>, 1997-2012.
- 2 J. R. Lakowicz, *Principles of Fluorescence Spectroscopy*, Kluwer Academic/Plenum Publishers, New York, London, Moscow, Dordrecht, 1999.
- 3 D. Magde, G. E. Rojas and P. G. Seybold, *Photochem. Photobiol.*, 1999, **70**, 737-744.